

# Aggregation Kinetics of *Meso*-tetrakis(4-sulfonatophenyl) Porphine in the Presence of Proteins: Temperature and Ionic Strength Effects

Suzana M. Andrade<sup>1,2</sup> and Silvia M. B. Costa<sup>1</sup>

Received September 27, 2001; revised December 17, 2001; accepted December 18, 2001

The kinetics of J-aggregation was studied through UV/Vis spectroscopy for *meso*-tetrakis(4-sulfonatophenyl) porphine—TSPP at pH = 2.0 using the protein human serum albumin as template. The effect of protein concentration on the kinetics was monitored by the appearance of the J-aggregate band at 486 nm and the simultaneous decrease of the monomer absorption at 434 nm. A simple equation based on the  $X \xrightarrow{k} Y$  reaction, where  $k$  may be assumed as a pseudo-first-order rate, fits well both the J-aggregation formation and monomer transformation. Temperature dependence of the reaction rate follows an Arrhenius behavior up to  $T = 38^\circ\text{C}$ , but above this value the dependence is inverted. This temperature seems to reflect the mid-point for the thermal denaturation of HSA. Ionic strength effect clearly exposes the prevalence of the electrostatic nature of this J-aggregation, and using a semi-empirical equation an estimate of the interaction length between TSPP- $\text{Na}^+$  of 4.5 Å was obtained in good agreement with crystallographic data. Absorption band shift and bandwidth were used to estimate the number of monomers in the J-aggregate unit that leads to spectral changes, and a number around 6–7 was found. There is no apparent growth of J-aggregate taking into account the invariance of the bandwidth of J-aggregate band with time at any of the temperatures studied.

**KEY WORDS:** Aggregation kinetics; porphyrin; human serum albumin; fluorescence; temperature; ionic strength.

## INTRODUCTION

Molecular self-assembling systems are a topic of keen activity because of their potential technological applications (as mesoscopic materials). Studies concerning molecular aggregation have focused mainly on cyanine dyes. More recently, interest has turned to aggregates of synthetic porphyrins. The excited state structure and properties of porphyrins may be used to gain insight on important biological processes such as energy transfer in

photosynthesis, photodynamic therapy of cancers, and interaction with proteins (hemeproteins). Depending on their electronic and stereochemical properties, porphyrins are able to self-assemble non-covalently into dimers or higher-ordered structures. In particular, *meso*-tetrakis(4-sulfonatophenyl) porphine—TSPP—was reported, under certain conditions of concentration, pH and ionic strength, to be able to form J-aggregates [1–3]. These correspond to the limiting case of parallel monomeric units staked edge-to-edge. In particular, TSPP J-aggregates are characterized by a side-by-side stacking structure of the zwitterionic porphyrins, exhibiting a sharp and narrow red-shifted band at 490 nm (in the B-band region) and another at 705 nm (in the Q-band region) [1–3]. Some controversy exists concerning the origin of a blue-shifted maxima

<sup>1</sup> Centro de Química Estrutural, Complexo 1, Instituto Superior Técnico, 1049-001 Lisboa Codex, Portugal.

<sup>2</sup> To whom correspondence should be addressed. Phone: (351) 21 8419389; Fax: (351) 21 8464455; e-mail: sandrade@popsrv.ist.utl.pt

appearing at 420 nm and attributed by some investigators [2–3] to the formation of H-aggregates, but also suggested to originate from different excitonic manifolds of the degenerated B state of TSPP [1,4].

Spectroscopic studies of porphyrins are important because of the close structural resemblance of their aggregates to the chlorophyll ones [5]. Study of interactions with proteins is directed to derive information concerning the physical properties of such aggregates to further understand the relationship between structure and biological activity.

In this work, the kinetics of the aggregation process was followed by UV/Vis absorption, taking advantage of the quite distinct spectral features of the monomeric and aggregated species. It is established that different regimes of aggregation kinetics may take place in colloidal systems depending on the inter-particle interaction potential, which can be controlled by the ionic strength or the pH.

The aggregation of TSPP also may be promoted by electrostatic interactions with oppositely charged material, forming confined media such as surfactants [3] or aluminosilicate mesostructure [6] acting as template supports. Recently, we investigated the effect of two drug carrier proteins, human serum albumin (HSA) and  $\beta$ -lactoglobulin ( $\beta$ LG), on TSPP. Under certain protein/porphyrin ratios (depending on the protein) and pH solution, J-aggregation of TSPP was detected [7]. This paper presents the kinetics of TSPP aggregation in the presence of HSA at different concentrations, and the protein's "catalytic" role is discussed from temperature and ionic strength effects.

## EXPERIMENTAL

### Materials

HSA fraction V, 96–99% purity (catalogue no. A-1653) was purchased from Sigma and used without further purification. TSPP was obtained from Fluka  $\geq 98\%$  purity (catalogue no. 88074). The probe concentrations were determined spectrophotometrically, considering the molar extinction coefficient  $\epsilon_{280nm}^{HSA} = 42864 \text{ M}^{-1} \text{ s}^{-1}$ ,  $\epsilon_{413nm}^{TSPP} = 5.0 \cdot 10^5 \text{ M}^{-1} \text{ s}^{-1}$  at pH = 6, the latter was always kept around 2  $\mu\text{M}$ . Buffer solutions were made up using bi-distilled water, following the recommended procedures. In all experiments we used fresh stock solutions of proteins and porphyrin in water. Stock aqueous solutions of TSPP were diluted by injection of a minimal quantity into a buffered protein solution, typically 3 ml, placed in a quartz cuvette of 1-cm path length, followed

by vigorous shaking such that the final TSPP concentration was  $\sim 2 \mu\text{M}$ .

### Methods

UV/Vis absorption measurements were made using a Jasco V-560 spectrophotometer thermostated by a circulating water bath. Stopped-flow kinetic data were obtained with a Hi-Tech model SFA-11 instrument. A Perkin-Elmer LS 50B spectrofluorimeter was employed in fluorescence measurements. The instrumental response at each wavelength was corrected by means of a curve obtained using appropriate fluorescence standards (until 400 nm) together with the one provided with the instrument. Fluorescence quantum yields of aerated solutions of TSPP were determined relative to that of TPP in toluene ( $\phi \approx 0.11$ ), with appropriate corrections for the refractive index of the solvent.

## RESULTS AND DISCUSSION

TSPP is water-soluble and exists as a monomer in aqueous solution below 30  $\mu\text{M}$ . Two chemical forms can be in equilibrium, because of protonation of the two pyrrolic nitrogen atoms in the porphyrato macrocycle ( $pK_a \sim 4.8$  at 25°C and  $\mu = 0.1$ ).

Although the absorption spectra of the deprotonated species,  $\text{TSPP}^{4-}$ , exhibits features of  $D_{2h}$  symmetry, at pH = 2 the symmetry increases to  $D_{4h}$ , featuring a shift of the Soret band from 413 to 434 nm and non-splitting of the Q-bands. In these acidic conditions, two new absorption bands may appear simultaneously at  $\approx 490$  nm and  $\approx 705$  nm, in parallel with the decrease of the correspondent Soret band and Q-band, Fig. 1. These two new bands have been assigned to the formation of J-aggregates in solution and are enhanced by increasing porphyrin concentration, ionic strength and/or acidity, and, as it will be explored in this paper, protein concentration. The zwitterionic form of  $\text{TSPP}^{2-}$  has been suggested as responsible for the formation of hydrogen bonds and electrostatic interactions that stabilize this type of aggregate [2,3].

### Protein Concentration Effects

The presence of HSA introduces remarkable changes in the spectroscopic features of TSPP (see Fig. 1). The protein possesses positive global charge ( $pK_a^{HSA} \approx 5.4$ ) in acidic conditions. So, at low pH (e.g., pH = 2.0) it may provide a positive microphase, distinct from the aqueous bulk, which induces TSPP aggregation in the

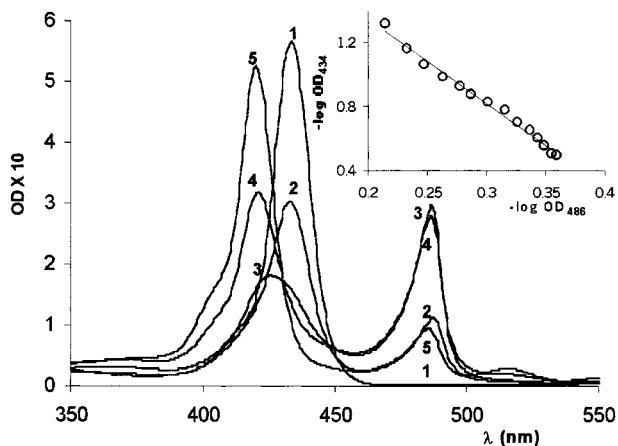


**Fig. 1.** Absorption spectra of TSPP in aqueous solution (2  $\mu\text{M}$ , pH = 2.0  $\mu \approx 0.025$ ), 1 – without protein and in the presence of HSA: 2 – 0.03  $\mu\text{M}$ ; 3 – 0.05  $\mu\text{M}$ ; 4 – 0.08  $\mu\text{M}$ ; 5 – 0.24  $\mu\text{M}$ ; 6 – 0.50  $\mu\text{M}$ . Insert: Plot of decimal logarithm of the OD at 434 versus that at 486 nm; the slope gives the magnitude of the aggregation number (see text).

presence of a submicromolar concentration of protein. This type of interaction must have an electrostatic character because at pH = 7.0, where the global charge of the protein is negative and the porphyrin is no longer a zwitterion but rather an anion, such J-aggregates are not detectable. As more protein is added to the solution the balance between electrostatic and hydrophobic mutual interactions is such that J-aggregates are no longer stabilised and a complex TSPP-protein prevails at both pH = 2.0 and pH = 7.0 [7].

J-aggregation kinetics of TSPP induced by the protein's presence was followed as a function of the concentration of the latter, at pH = 2.0 in buffered aqueous solutions, and a very well-defined isosbestic point was found at  $\lambda \approx 449$  nm (Fig. 2A). The insert in Fig. 2A displays the build-up of J-aggregates (as monitored by the absorbance at 486 nm, which is almost entirely due to this aggregate) with time at different protein concentrations. Contrary to data obtained for TSPP aggregation in the presence of 0.3 M HCl [8], no lag or induction period is observed. Usually, an induction period is characteristic of autocatalysis, that is J-aggregate already formed induces the build-up of more. This induction period tends to decrease with the increase of the concentration of associative species. Nevertheless, the authors managed to avoid such period by changing the sample preparation procedure, which seems, at first sight, to be responsible for the different behavior found. Whereas more complicated equations are necessary to account for the spontaneous formation of such a “critical” aggregation nucleus, in our case simpler equations were used successfully. Assuming a “catalytic” role for the protein (E), a possible

reaction scheme could involve two consecutive (pseudo) first-order reactions, such as:



provided that the back reaction of XE to the reagents is negligible. If  $[X] \gg [E]$ , then the first step in the reaction sequence has pseudo-first-order kinetics.

Assuming the absorption obtained at 434 nm and at 486 nm as representative of the species present in solution for the range of protein concentrations used, then the set of equations expressing the species concentration as a function of time shows that a simpler kinetic scheme may be used where  $X + E \xrightarrow{k'} E + Y$ , and Eq. 2 can describe both the kinetics of monomer consumption and J-aggregate formation,

$$OD^\lambda = \epsilon_X^\lambda [X]_0 \exp(-kt) + \epsilon_J^\lambda [X]_0 \{1 - \exp(-kt)\} + \epsilon_J^\lambda [J]_0 \quad (2)$$

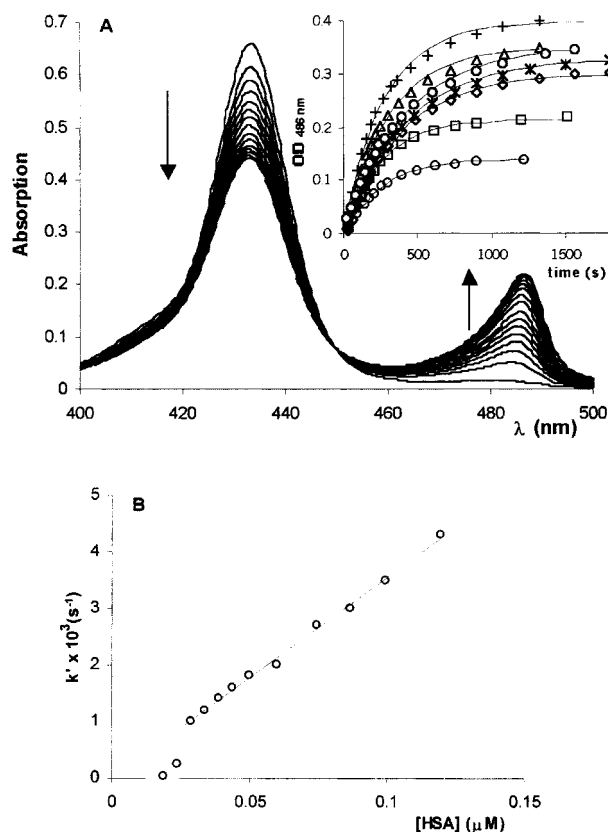


**Fig. 2.** (A) Time evolution of the absorption spectra of TSPP (2  $\mu\text{M}$ ) in buffered solutions (pH = 2.0) containing 0.03  $\mu\text{M}$  of HSA. Insert: Kinetics of the absorption of TSPP J-aggregate in the presence of different concentrations of HSA range: 0.02  $\mu\text{M}$ –0.12  $\mu\text{M}$ ; full lines represent the best fit using Eq. (2). (B) Dependence of pseudo-first-order rate constant obtained using Eq. (2) on the protein concentration.

where  $\epsilon_x$  and  $\epsilon_j$  are the extinction coefficients, respectively, of the monomer and J-aggregate. Rate constants obtained at  $\lambda = 486$  nm or at  $\lambda = 434$  nm are relatively close, for example,  $k'_{486} = 1.82 \times 10^{-3} \text{ s}^{-1}$  and  $k'_{434} = 2.44 \times 10^{-3} \text{ s}^{-1}$  at  $[\text{HSA}] = 0.05 \text{ } \mu\text{M}$ . The fact that  $k'_{434}$  is higher than  $k'_{486}$  could imply that there is an overlap of the absorption spectra of monomer and J-aggregates in the region of 434 nm, or that the aggregation mechanism could involve intermediate species. Nevertheless, the fits are good at all protein concentrations tried and at both wavelengths and are roughly close to the values obtained in 0.3 M of HCl [8]. Also, a good agreement ( $\pm 20\%$ ) exists when comparing kinetic data obtained using hand-mixing and stop-flow techniques. A plot of  $k'$  is linearly dependent on the protein initial concentration (Fig. 2B) and a true constant of  $3.5 \times 10^{-2} \text{ } \mu\text{M}^{-1} \text{ s}^{-1}$  is obtained.

### Temperature Effects

The effect of temperature on the kinetics of J-aggregation was followed at four different HSA concentrations in the range of 10–48°C. This aggregation process occurs via HSA presence; thus it is natural that the thermal stability of the protein may influence the kinetics. It is known that proteins themselves may undergo a deactivation process that has a high activation energy. As a result, the rates of enzyme-catalysed reactions frequently pass through a maximum as the temperature is raised. Indeed, this is observed for all the protein concentrations studied. Figure 3A shows a similar behavior, where a maximum for  $k'$  is obtained at  $T \approx 37.8^\circ\text{C}$ . A fluorescence study of HSA sole tryptophan residue ( $\text{Trp}^{214}$ ) (Fig. 4) led to a transition temperature of  $\approx 40.6^\circ\text{C}$  (if we assume a two-state model for the protein thermal unfolding, this temper-

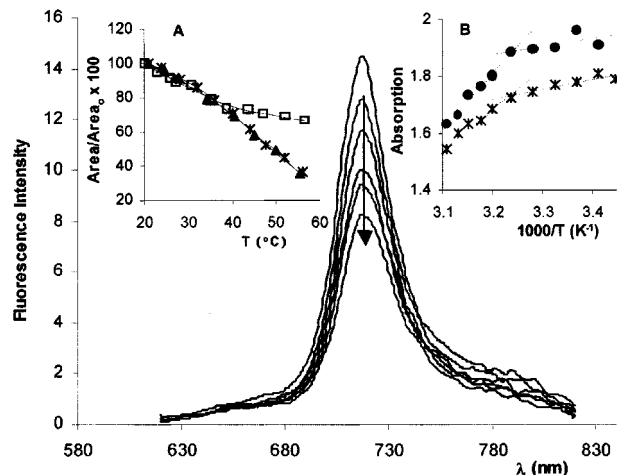


Fig. 4. Fluorescence intensity of TSPP in the presence of HSA ( $0.1 \text{ } \mu\text{M}$ ) at different temperatures from  $20^\circ\text{C}$ – $50^\circ\text{C}$  (as indicated by the arrow),  $\lambda_{\text{exc}} = 490$  nm. Insert (A) Temperature dependence of the area under the fluorescence spectra of TSPP/HSA obtained at  $\lambda_{\text{exc}} = 296$  nm (\*),  $430$  nm ( $\blacktriangle$ ), and  $490$  nm ( $\square$ ). Insert (B) Temperature dependence of TSPP ( $2 \text{ } \mu\text{M}$ ) absorption at  $434$  ( $\circ$ ) and at  $490$  (\*) in the presence of HSA.

ature corresponds to a point where half of it is in the native state and the other half is unfolded.) The presence of TSPP did not introduce a significant conformational change on the protein's tertiary structure, accounting for the similar transition temperature (insert A of Fig. 4), and only a decrease in the unfolding enthalpy and entropy is obtained. Thus TSPP presence does not introduce an increase in  $\text{Trp}^{214}$  aqueous exposure. The effect of temperature on the system TSPP( $2 \text{ } \mu\text{M}$ )/HSA( $0.05 \text{ } \mu\text{M}$ ) at  $\text{pH} = 2.0$ , can be followed by plotting the absorption at the maxima of both the Soret band ( $434$  nm) and J-aggregate band ( $486$  nm). A breaking point is detected at  $T \approx$

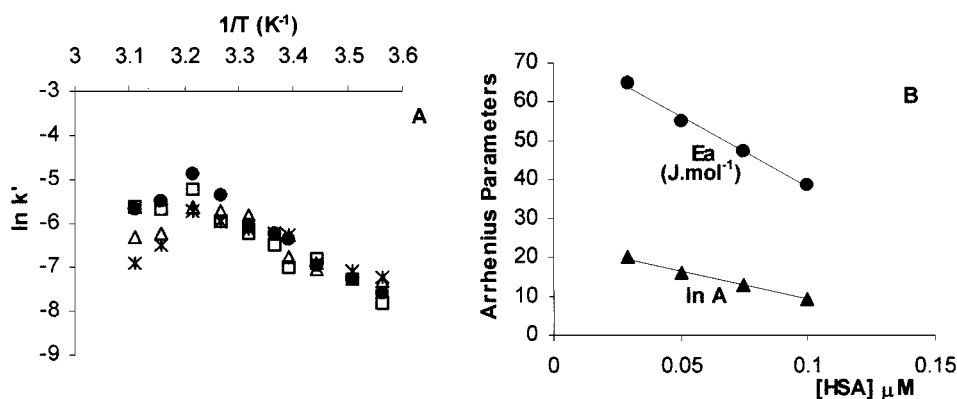


Fig. 3. Arrhenius plots of pseudo-first-order rate constant obtained using Eq. (2) ( $\lambda = 486$  nm) at different HSA concentrations:  $\bullet$ :  $0.03 \text{ } \mu\text{M}$ ;  $\blacksquare$ :  $0.05 \text{ } \mu\text{M}$ ;  $\triangle$ :  $0.075 \text{ } \mu\text{M}$ ;  $*$ :  $0.1 \text{ } \mu\text{M}$ . (B) Arrhenius parameters obtained for the J-aggregation kinetics read at  $486$  nm as a function of HSA concentration.

37.0°C in both cases (insert B of Fig. 4). Overall, the results seem to point to an alteration in the TSPP interaction with the protein as a result of small changes in the protein's conformation caused by thermal denaturation.

The influence of temperature on the rate of a reaction is usually interpreted in terms of the Arrhenius equation,  $k = A \exp(-E_a/RT)$ , where  $A$  is the preexponential factor and  $E_a$  the activation energy. The analysis of Fig. 3B shows that there is an indication that large protein concentrations need less energetic encounters for the reaction to occur. The plot of  $\ln k'$  vs.  $1/T$  is linear up to  $T \leq 38^\circ\text{C}$ , following the predicted Arrhenius pattern. The extracted values of  $E_a$  and  $A$  for each HSA concentration were plotted against the latter, and a linear dependence was also obtained. At  $T \geq 38^\circ\text{C}$  an inverted temperature dependence is observed with both  $\Delta H_{\text{obs}}^\ddagger$  and  $\Delta S_{\text{obs}}^\ddagger$  negative, according to the well-known Eyring equation. Therefore the temperature increase above  $38^\circ\text{C}$  seems to result in a more favorable and accessible electrostatic environment for TSPP aggregation to occur as a result of changes in the protein folding.

**Electrostatic Effects**

Absorption data at constant ionic strength shows that the absorption at 490 nm (and 705 nm) decreases with increasing pH, disappearing at  $\text{pH} > \text{pK}_a$ , for  $[\text{TSPP}] = 2 \mu\text{M}$  [7]. While at constant pH (below  $\text{pK}_a$ ) the ionic strength gives rise to a decrease in the monomer Soret band absorption, and an initial increase in the J-aggregate absorption band, followed by a small decrease, a red-shift, and a band broadening (Fig. 5A) of the latter have been ascribed to the presence of different sized aggregates [3]. Fluorescence emission (Fig. 5B) shows a single maxima at 670 nm characteristic of the monomer in water at  $\text{pH} = 2.0$ , while the presence of NaCl leads to the quenching of such band and the appearance of a band centered at  $\approx 720 \text{ nm}$ , which follows a pattern similar to the J-aggregate absorption band at 490 nm. As mentioned before, electrostatic interactions are expected to play a major role because TSPP carries a global two-unit negative charge and HSA is highly positive below their isoelectric point. At neutral pH all species are negatively charged, and consequently the ionic strength makes TSPP-protein binding more favorable and a complex is denoted (Soret band shift 413–422 nm at  $\text{pH} = 7.0$  [6], and Soret band shift from 434 nm to 422 nm at  $\text{pH} = 2.0$ , [see Fig. 1]). It is therefore reasonable to assume that the effective free energy for the association process arises from two contributions, an electrostatic interaction with a Debye-Hückel screening term dependent on the square root of ionic strength (the major contribution at

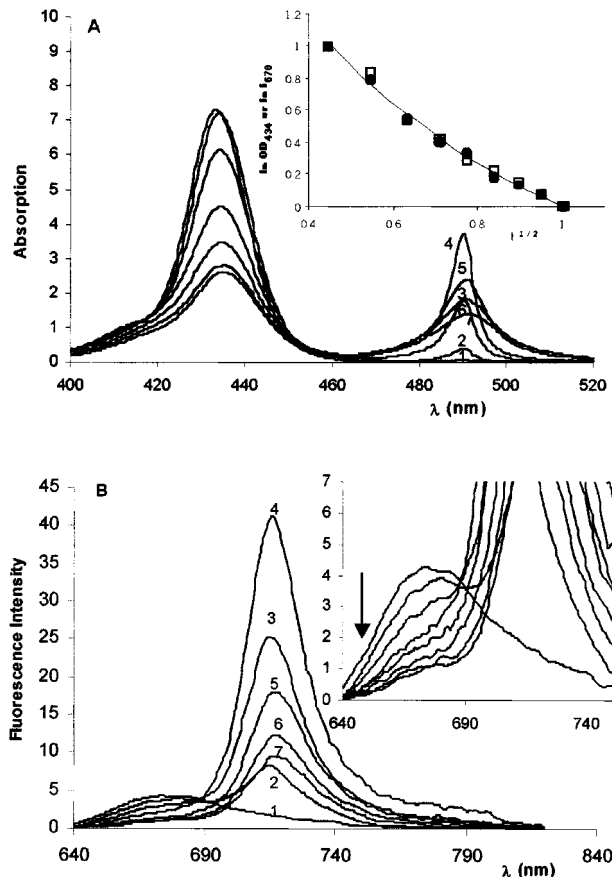


Fig. 5. Ionic strength effect on (A) TSPP absorption and (B) TSPP fluorescence ( $\lambda_{\text{exc}} = 490 \text{ nm}$ ,  $[\text{TSPP}] = 2 \mu\text{M}$ ,  $\text{pH} = 2.0$ ),  $[\text{NaCl}] = 0 - 1 \text{ M}$ . Insert (A): Natural logarithm of TSPP absorption Soret band at 434 nm and fluorescence intensity at 670 nm versus square root of ionic strength in molar units. Full line represents the best fit using Eq. (3).

pH below  $\text{pK}_a$ ) and a non-electrostatic term including all other interactions probably prevailing at pH above  $\text{pK}_a$ . Thus an empirical equation, Eq. (3), may be written:

$$\ln(\text{OD}) = A + B \exp(-CI^{1/2}) \quad (3)$$

where  $A$  contains non-electrostatic interactions,  $B$  is the electrostatic term, and  $C$  is the Debye screening. This equation fits also reasonably well the monomer fluorescence intensity at 670 nm (insert Fig. 5A), with the values  $A = 0.25$ ;  $B = 3.6$ ; and  $C = 1.6$ . The  $B$  value obtained clearly underlines the domain of electrostatic interactions under the conditions studied. Because TSPP is a zwitterionic molecule, the positively charged centers attract the negatively charged peripheral substituents of the adjacent molecules. Excess cations (either  $\text{Na}^+$  or  $\text{H}^+$ ) screen the repulsions of the anionic sulfonate groups of adjacent molecules. A rough estimate of the TSPP- $\text{Na}^+$  interaction length of  $4.5 \text{ \AA}$  (based on  $C$  value) is close to geometric parameters recovered from crystallographic data [4].

### Aggregate Size

There is still no method to determine accurately the size  $N$  of a J-aggregate. DLS experiments [9] showed the existence of polydisperse clusters, the small ones averaging 3–6 nm led to an aggregation number of 6–32 TSPP molecules, together with larger clusters of 100–200 nm and others in the 1–1.5  $\mu\text{M}$  range. The number of molecules in a given J-aggregate can be inferred from spectral properties—band shift and bandwidth [10]—or from the OD at both monomer and J-aggregate band maxima [11]. The approximate values obtained from our data— $N \approx 7$  from spectral shift,  $N \approx 8$  obtained from bandwidth, and  $N \approx 6$  from OD values at 434 and 490 nm [insert, see Fig. 1]—are slightly higher than that obtained in the presence of CTAB ( $N \approx 5$ ) [3]. As a comparison, one has to take into account that  $N$  values obtained through spectral changes report the number of consecutive neighbor molecules that are collectively excited. This number must be conditioned by the positive surface of the protein domain that supplies the suitable environment for such aggregation process. Such area must be higher for the protein than for the aqueous micelle accounting for the differences found.

The bandwidth of the J-aggregate band did not change with time at any of the temperatures studied, and the band shift was not higher than 3 nm to the red in any case. This seems to indicate that there is no apparent growth of J-aggregates, which would lead to inhomogeneous broadening and increase of FWHM of the J-band.

### CONCLUSIONS

Data gathered here clearly shows that the presence of HSA induces TSPP aggregation, under acidic conditions.

These J-aggregates are formed from monomers of TSPP following a simple kinetic model. The rates extracted show an Arrhenius behavior up to  $T \approx 38^\circ\text{C}$ , above which an inverted situation occurs. This temperature agrees well with the temperature at which thermal unfolding of the protein is found.

Ionic strength emphasizes the electrostatic nature of the interactions leading to TSPP aggregation.

### ACKNOWLEDGEMENTS

This work was supported by Project POCTI/35398/QUI/2000. S. M. Andrade thanks FCT for BPD grant no. 18855. The authors thank Mr. P. Sanches for help in the temperature experiments.

### REFERENCES

1. O. Ohno, Y. Kaizu, and H. Kobayashi (1993) *J. Chem. Phys.* **99**, 4128–4139.
2. D. L. Akins, H.-R. Zhu, and C. Guo (1994) *J. Phys. Chem.* **98**, 3612–3618.
3. N. C. Maiti, S. Mazumdar, and N. Periasamy (1998) *J. Phys. Chem. B* **102**, 1528–1538.
4. D.-M. Chen, T. He, D.-F. Cong, Y.-H. Zhang, and F.-C. Liu (2001) *J. Phys. Chem. A* **105**, 3981–3988, and reference cited therein.
5. H. Kano, T. Saito, and T. Kobayashi (2001) *J. Phys. Chem. B* **105**, 413–419.
6. W. Xu, H. Guo and D. L. Akins (2001) *J. Phys. Chem. B* **105**, 1543–1546.
7. S. M. Andrade and S. M. B. Costa (2002) *Biophys. J.* **82**, 1607–1619.
8. R. F. Pasternack, C. Fleming, S. Herring, P. J. Collings, J. dePaula, G. DeCastro, and E. J. Gibbs (2000) *Biophys. J.* **79**, 550–560.
9. N. Micali, F. Mallamace, A. Romeo, R. Purrello, and L. M. Scolaro (2000) *J. Phys. Chem. B* **104**, 5897–5904.
10. K. Kemnitz, K. Yoshihara, and T. Tani (1990) *J. Phys. Chem.* **94**, 3099–3104.
11. A. S. Tatikolov and S. M. B. Costa (2001) *Chem. Phys. Lett.* **346**, 233–240.